

In Situ Compatibilized SAN/LCP Blends Through Reactive Copolymers

JIEH-MING HUANG,¹ MIN-FENG YOU,² FENG-CHIH CHANG³

¹ Department of Chemical Engineering, Van Nung Institute of Technology, Chung-Li 32054, Taiwan

² Chemical Research Division, Chung Shan Institute of Science and Technology, Lungtan 32526, Taiwan

³ Institute of Applied Chemistry, National Chiao-Tung University, Hsinchu 30043, Taiwan

Received 8 December 2000; accepted 15 March 2001

ABSTRACT: Styrene–acrylonitrile–glycidyl methacrylate (SAG) copolymers with various contents of glycidyl methacrylate (GMA) were used to compatibilize the incompatible blends of styrene–acrylonitrile (SAN) and a liquid crystalline polymer (LCP). These SAG copolymers contain reactive glycidyl groups that are able to react with the carboxylic acid and/or hydroxyl end groups of the LCP to form the SAG-*g*-LCP copolymers during melt processing. The *in situ*-formed graft copolymers tend to reside along the interface to reduce the interfacial tension and to increase the interface adhesion. The morphologies of the SAN/LCP blends were examined by using scanning electron microscopy (SEM), where the compatibilized SAN/LCP blends were observed with greater numbers and finer fibrils than those of the corresponding uncompatibilized blends. The mechanical properties of the blends increased after compatibilization. The presence of a small amount (200 ppm) of ethyl triphenylphosphonium bromide (ETPB) catalyst further promotes the graft reaction and improves the compatibilization. © 2001 John Wiley & Sons, Inc. *J Appl Polym Sci* 82: 3321–3332, 2001

Key words: polymer blend; SAN; LCP; reactive compatibilizer

INTRODUCTION

Polymer blends between thermoplastics (TPs) and liquid crystalline polymers (LCPs) have attracted much attention during the last decade.^{1–5} The use of LCPs in polymer blends looks attractive from a number of viewpoints. First, their inherent rigid molecular structure gives polyblends with good mechanical properties. Second, LCPs have low melt viscosity, thus allowing good flow properties and improving the processing of

the blends. Other useful properties include high chemical resistance and low thermal expansion coefficient, which results in low mold shrinkage. Therefore, two major advantages gained by the addition of a small amount of LCP to thermoplastic polymers are processability improvement and enhancement on mechanical properties, especially for modulus and tensile strength in the machine direction.

However, most TP/LCP blends are considered to be immiscible and incompatible with poor interfacial adhesion. This result leads to the polyblends having low tensile strength and modulus when compared with theoretically predicted values. To increase compatibility between LCP and thermoplastics, graft polymers or copolymers

Correspondence to: F.-C. Chang (changfc@cc.nctu.edu.tw).
Contract grant sponsor: National Science Council, Republic of China.

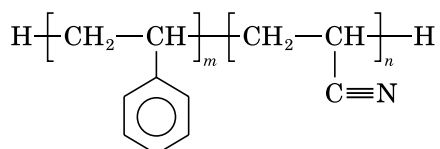
Journal of Applied Polymer Science, Vol. 82, 3321–3332 (2001)
© 2001 John Wiley & Sons, Inc.

have been introduced in TP/LCP blends. For example, Baird and coworkers^{6,7} reported that the adhesion between the LCP and polypropylene (PP) matrix is significantly improved by the presence of maleic anhydride-grafted polypropylene, which acts as an effective compatibilizer. Tjong and Xie⁸ studied the effect of styrene-maleic anhydride (SMA) copolymer on the properties of polyamide-6 (PA6)/LCP blends. They found that the stiffness, tensile strength, and toughness of the *in situ* composites are generally improved with increasing SMA content. However, these mechanical properties deteriorated considerably when the SMA content was above 10 wt %. In a continuous program to investigate the *in situ* compatibilization of polyblends, we have reported a series of reactive compatibilized blends based on GMA-containing copolymers involving the following polymer pairs: polystyrene (PS)/poly(ethylene terephthalate) (PET),⁹ PS/poly(butylene terephthalate) (PBT),¹⁰ acrylonitrile-butadiene-styrene (ABS)/phenoxy,¹¹ ABS/nylon 6,6,¹² ABS/PBT,¹³ Noryl/LCP,¹⁴ and PS/LCP.¹⁵ In this study, we report SAG-compatibilized polymer blends of SAN and LCP, their miscibility, morphology, and correlation with their mechanical properties.

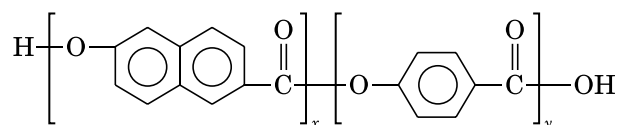
EXPERIMENTAL

Materials

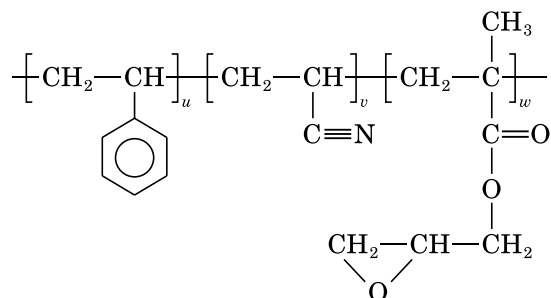
SAN (trade name KIBISAN) was kindly supplied by Chi-Mei Corp. of Taiwan. It is a copolymer of 76% styrene and 24% acrylonitrile. The LCP (Vectra A900) used is an aromatic copolyester consisting of 73% 4-hydroxybenzoic acid and 27% 2-hydroxy-6-naphthoic acid, supplied by Hoechst Celanese Corp. SAG copolymers with 2, 5, and 8% glycidyl methacrylate (GMA) and constant styrene/acrylonitrile ratio ($S/A = 65/25$) were prepared by suspension polymerization, the detailed procedures of which were previously described.^{9,13} The catalyst employed in this study, ethyl triphenylphosphonium bromide (ETPB), was obtained from Merck. The materials used have the following structure:



Styrene-acrylonitrile copolymer (SAN)



Thermotropic liquid crystalline polymer (LCP)



Styrene-acrylonitrile-glycidyl methacrylate copolymer (SAG)

Melt Blending and Specimen Preparation

All blends were prepared in a 30-mm corotating twin-screw extruder by maintaining the barrel temperature in the range of 280–300°C and the screw speed at 260 rpm. The extruded pellets were dried at 120°C for over 10 h and then molded into standard ASTM specimens by an Arburg 3-oz injection-molding machine (Germany).

Torque versus Time Measurements

To verify the reaction between SAG and LCP based on the viscosity increase, 40 g of sample (weight ratio = 1 : 1) was tested at 285°C and 30 rpm in a Brabender Plasti-Corder (Germany).

Characterizations

Melt flow rates (MFRs) of base polymers and blends were measured at 300°C using a 2.16-kg loading by an automatic flow rate timer from Ray-Ran Corp. (UK). The capillary rheological measurements were carried out at 300°C using a capillary rheometer ($L/D = 40$, orifice radius = 0.02 in.) from Kayeness Corp. (Pennsylvania). Morphologies of the cryogenically fractured surfaces of the injection-molded specimens were examined from core to skin regions, parallel to the flow direction, by scanning electron microscopy (SEM) using a model S-570 from Hitachi Corp. (Tokyo, Japan). Standard tensile tests were conducted by following the ASTM-D638 method at ambient conditions with a crosshead speed of 5 mm/min. Unnotched Izod impact strength were measured

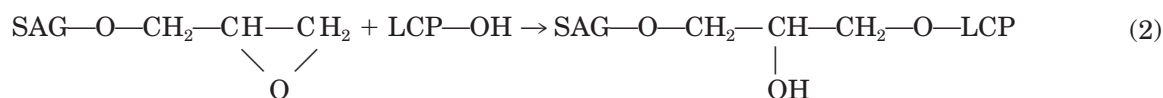
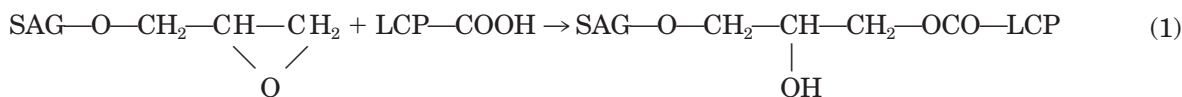
at ambient conditions according to the ASTM-D256 method.

RESULTS AND DISCUSSION

Fundamentals of *in Situ* Compatibilization

An *in situ* reactive compatibilizer is a copolymer containing reactive functional groups that are able to react with blend components to form a copolymer and to act as a compatibilizer. The content and structure of an *in situ* compatibilizer will vary with the amount of the reactive groups, temperature, time, mixing efficiency, and presence of a catalyst. Therefore, this type of compatibilizer is considered as a nonspecific type compatibilizer. In this study, the reactive copolymer (SAG) itself cannot act as a phase compatibilizer for the polyblends of SAN and LCP. However, the reaction products between the epoxide groups in

the SAG copolymer and the $-\text{COOH}$ or $-\text{OH}$ end groups of the LCP will produce various SAG-*g*-LCP copolymers that will function as nonspecific compatibilizers. An excessive reaction between SAG and LCP will result in the highly branched SAG-*g*-LCP copolymers or even a crosslinked network. Such an excessively grafted copolymer becomes too bulky and has the branched LCP chains effectively shielding off the styrene-acrylonitrile segments of the SAG copolymer, thus losing its role as a phase compatibilizer. Therefore, the optimized content of the *in situ*-formed copolymer is essential to achieve the greatest performance of the resulting blend products. This can be accomplished through proper adjustment of the GMA content in the SAG copolymer, the presence of a suitable catalyst, and proper control of the blending conditions. The reaction between the SAG copolymer and LCP end groups can be expressed by the following equations:



Melt Flow Rates (MFRs)

Table I summarizes the MFRs of the matrices and blends measured at 300°C with a load of 2.16 kg. Without the presence of compatibilizer, the SAN/LCP blends show higher MFR, as would be expected. Moreover, the uncompatibilized blend with greater LCP content (e.g., SAN/LCP = 80/20) results in higher MFR (lower viscosity). It is well known that the LCP in the thermoplastic matrix is able to reduce its viscosity. On the other hand, the trend clearly shows the decrease in MFR (molar mass increase) after compatibilization from all the compositions. The MFR is further decreased when the blend contains both SAG and 200 ppm of the ETPB catalyst. It has been well recognized that the epoxy group in the SAG copolymer is able to react with LCP end groups at interface to form SAG-*g*-LCP copolymers, which tend to anchor along the SAN/LCP interface. The molecular weight increase through grafting reaction is believed to be the major contributor for the viscosity increase of the blends. The increase of

the interfacial friction of the compatibilized blend over that of the uncompatibilized one is another reason for the observed higher viscosity.

Torque versus Time

Torque measurements were successfully utilized to obtain qualitative information concerning the chemical reactivity and the extent of the reactions in compatibilized blends.^{16,17} Figure 1 gives the torque versus time curves for the LCP, SAG8, LCP/SAG8 (50/50), and LCP/SAG8/Cat (50/50/0.02) blends. Both the LCP and SAG8 show a continuous and gradual decrease in torque with time, implying that slight thermal degradation probably occurs under the testing conditions. This result also indicates that the potential self-curing reaction of SAG8 does not occur. In contrast, the torque values of the mixtures of LCP/SAG8 and LCP/SAG8/Cat both increase significantly after about 40 s. The presence of 200 ppm catalyst in the mixture exerts a more pronounced effect of increasing the torque value. This observed increase of torque value can be attributed to the

Table I Melt Flow Rates of the SAN/LCP/SAG Blends^a

Composition	MFR (g/min)
SAN	53.6
LCP	71.8
SAN/LCP = 95/5	56.1
SAN/LCP = 90/10	60.5
SAN/LCP = 80/20	68.6
SAN/LCP/SAG2 = 90/10/1	58.5
SAN/LCP/SAG2/Cat = 90/10/1/0.02	56.4
SAN/LCP/SAG2 = 90/10/3	55.2
SAN/LCP/SAG2/Cat = 90/10/3/0.02	51.1
SAN/LCP/SAG2 = 90/10/5	54.0
SAN/LCP/SAG2/Cat = 90/10/5/0.02	48.6
SAN/LCP/SAG5 = 90/10/1	57
SAN/LCP/SAG5/Cat = 90/10/1/0.02	55.4
SAN/LCP/SAG5 = 90/10/3	54.8
SAN/LCP/SAG5/Cat = 90/10/3/0.02	54.3
SAN/LCP/SAG5 = 90/10/5	48.4
SAN/LCP/SAG5/Cat = 90/10/5/0.02	47.1

^a Tested at 300°C with a load of 2.16 kg.

molecular weight increase from the anticipated graft reactions between the LCP and SAG8. These *in situ*-formed graft copolymers are preferably distributed along the interface in the SAN/LCP blends to act as a compatibilizer of the blends.

Capillary Rheometry

Figure 2 shows the variation of shear viscosity with shear rate for pure LCP and SAN measured

at 290°C. Both the LCP and SAN show a non-Newtonian behavior within the shear rate investigated. From Figure 2, it is apparent that the LCP possesses a higher viscosity than that of the SAN under the same conditions, in spite of the LCP showing a more shear thin behavior. On the contrary, the LCP copolyester exhibits a lower shear viscosity when measured at 300°C and the shear rate is higher than 500 s⁻¹, as shown in Figure 3. For facilitating the formation of LCP fibrils, it is generally believed that the LCP component should possess a lower viscosity relative to that of the matrix.¹⁸ Figure 4 compares the shear viscosity versus shear rate plots at 300°C for the uncompatibilized and compatibilized SAN/LCP (90/10) blends with different contents of GMA in SAG copolymers. The uncompatibilized SAN/LCP blend has the lowest shear viscosity and the viscosity increases significantly after compatibilization. Furthermore, higher GMA content in SAG results in higher shear viscosity of the blend. For the uncompatibilized blend, a “slide” takes place easily between phases of two immiscible homopolymers under shear stress as a result of higher interfacial tension and lower interfacial friction. This phenomenon leads to the lowest viscosity of the uncompatibilized blend. In contrast, higher interfacial friction of the compatibilized blend is caused by the SAG-*g*-LCP copolymer anchoring along the interface and results in higher viscosity compared with that of the uncompatibilized blend. Figure 5 shows the shear viscosity versus shear rate plots for the uncompatibilized

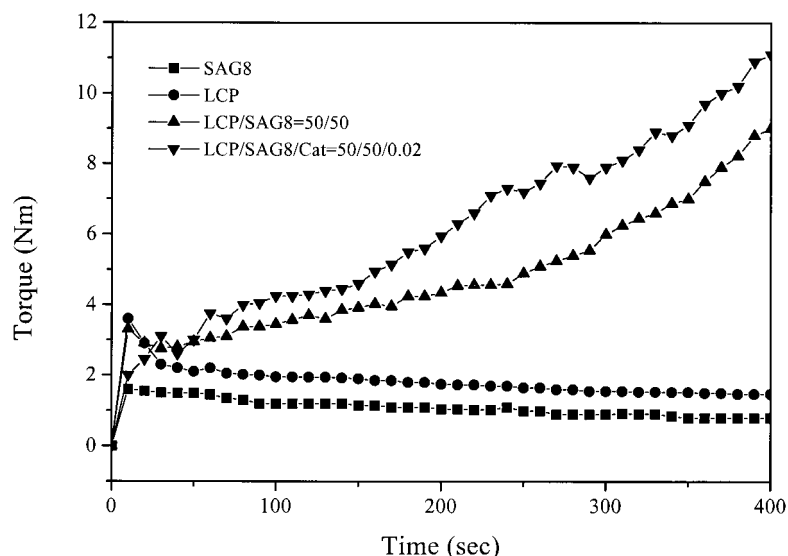


Figure 1 Plots of torque versus time for LCP, SAG8, and LCP/SAG8 blends.

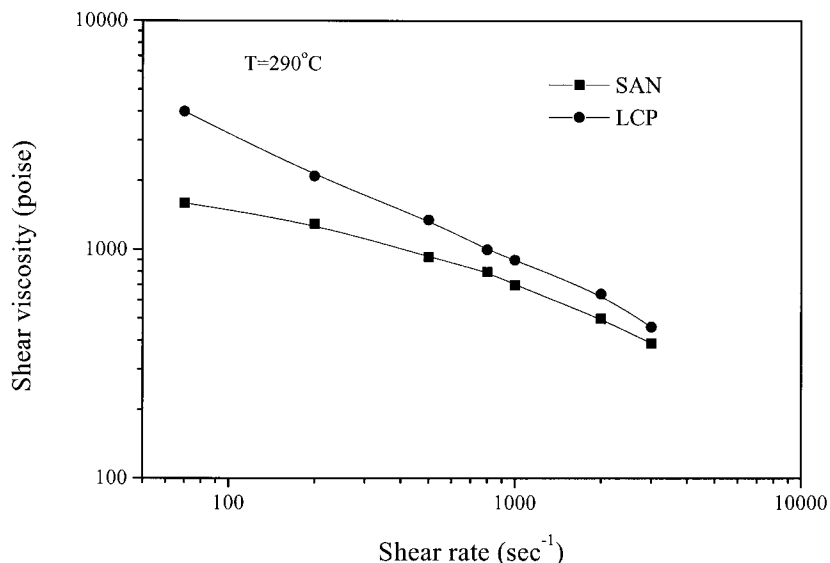


Figure 2 Plots of shear viscosity versus shear rate for SAN and LCP at 290°C.

and compatibilized SAN/LCP (90/10) blends with different SAG2 contents in the blend. The observed trend is similar to the MFR data, in which the better compatibilized blend results in higher viscosity. The presence of 200 ppm ETPB catalyst in the blend shows a further viscosity increase. The increase of viscosity can be attributed to the molecular weight increase and the enhancement of interfacial friction, as discussed earlier.

Effect of Shear Rate on Fibril Formation

The strings collected from the capillary rheometrical measurements at different shear rates

were used to investigate the effect of shear rate on the LCP fibril formation. Figure 6 shows the SEM micrographs of the uncompatibilized SAN/LCP (90/10) blend under different shear rates of 200, 500, and 1000 s⁻¹, respectively. For the lowest shear rate used ($\gamma = 200 \text{ s}^{-1}$), no LCP fibrillar structure is formed [Fig. 6(a)]. At higher shear rates ($\gamma \geq 500 \text{ s}^{-1}$), certain LCP fibrils can be clearly observed in these blends [Fig. 6(b) and (c)]. The highest shear rate employed in this study is somewhere between the typical extrusion and injection processings. To form the LCP fibrils in a TP/LCP blend with a fixed LCP content, a critical

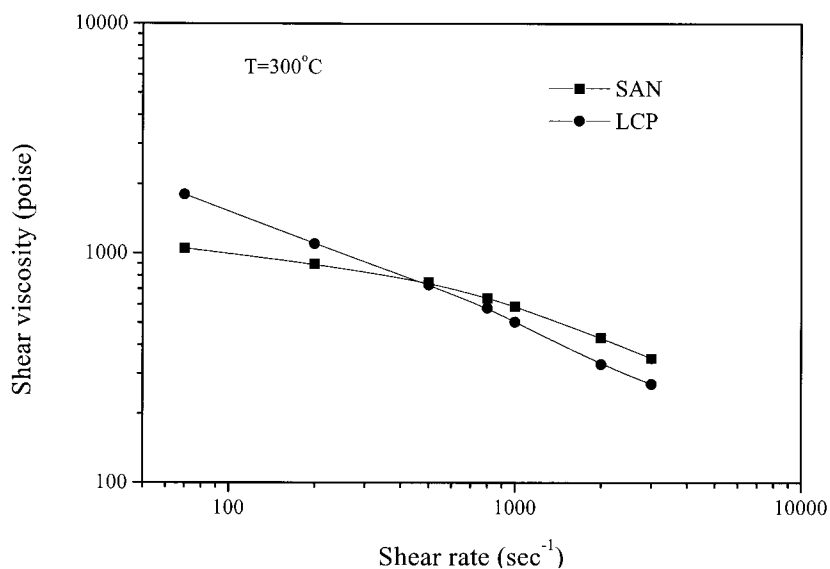


Figure 3 Plots of shear viscosity versus shear rate for SAN and LCP at 300°C.

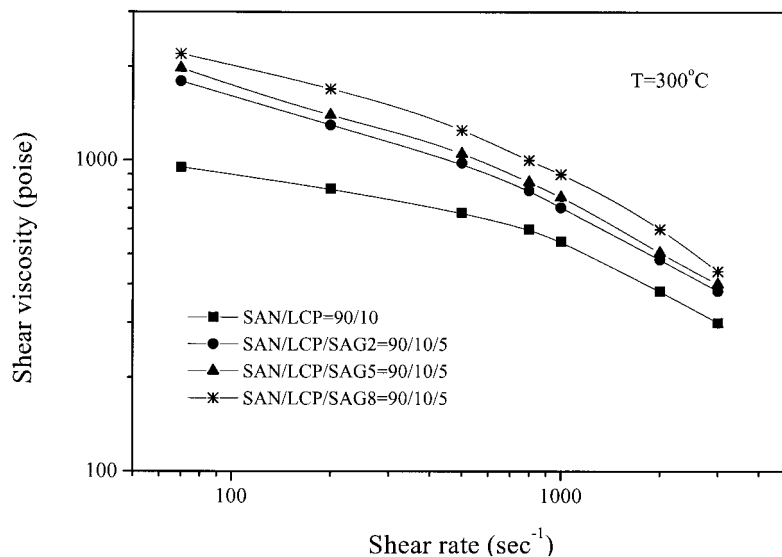


Figure 4 Plots of shear viscosity versus shear rate at 300°C for the uncompatibilized and compatibilized SAN/LCP/SAG (90/10/5) blends containing varying GMA contents.

shear rate must be reached. As mentioned earlier (Fig. 3), the viscosity of the LCP is lower than that of the SAN matrix when the shear rate is higher than 500 s^{-1} .

Scanning Electron Microscopy (SEM) Morphologies

The LCP phase in a TP/LCP blend usually exhibits a unique skin-core morphology perpendicular to the flow direction of the injection-molded specimen. The size, shape, and distribution of the LCP

domains depend on many factors such as composition, viscosity ratio of the component polymers, interfacial tension, the rheological characteristics of the matrix polymer, and the processing conditions. Highly oriented LCP fibrils are formed near the skin region, resulting from the elongational flow at the advancing flow front, whereas a less-oriented LCP domain at the core region is usually observed arising from the relatively lower shear flow at the center of the mold.¹⁹ Figure 7 shows

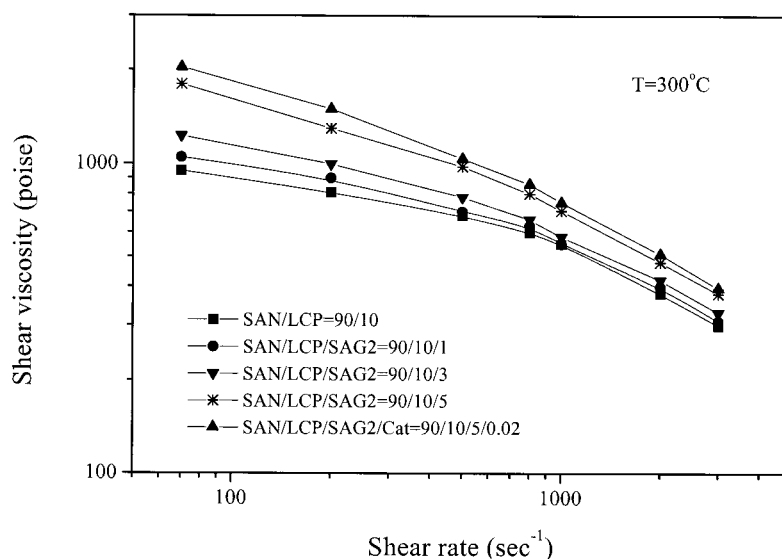


Figure 5 Plots of shear viscosity versus shear rate for the uncompatibilized and compatibilized SAN/LCP (90/10) blends containing varying amounts of SAG2 at 300°C.

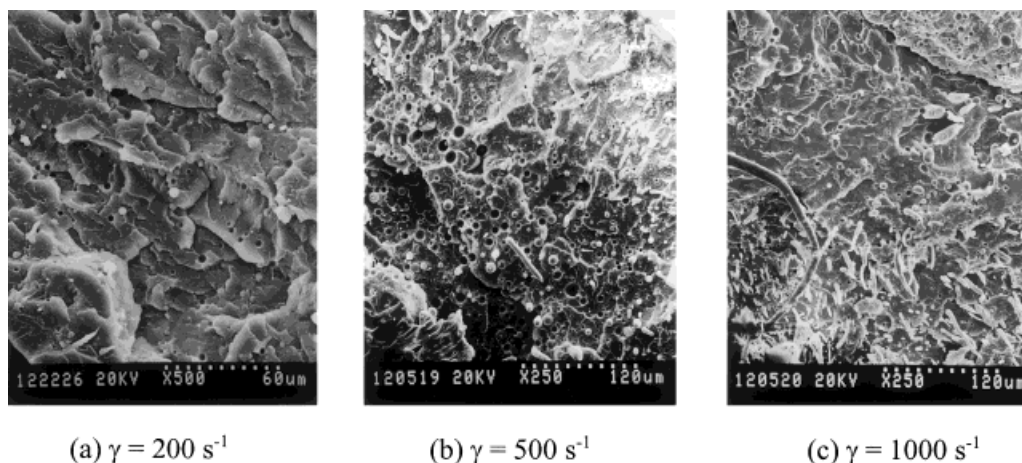


Figure 6 SEM micrographs of the SAN/LCP (90/10) blend under different shear rates.

SEM micrographs of the cryogenically fractured surfaces of the SAN/LCP (95/5) blend at different locations from core to skin of the injection-molded specimen. At the core region [Fig. 7(a)], the LCP phase domains are mainly in spherical droplets because the shear stress is not high enough to overcome the interfacial tension. At the quarter region, the midpoint between the central line and skin of the specimen, an elongated LCP domain can be observed, as shown in Figure 7(b). Eventually, in Figure 7(c), some fibrils with high aspect ratio are observed at the skin region, where the greatest shear gradient takes place.

Figure 8 shows the uncompatibilized and compatibilized SAN/LCP (90/10) blends with varying

SAG2 content observed at the core region. It is obvious that the uncompatibilized SAN/LCP blend exhibits relatively larger spherical LCP domains. The spherical domain size is reduced with increasing the amount of SAG2 in the blend, indicating the improvement of the compatibilization of the SAN/LCP blends. Figure 9 displays the effect of SAG2 content on the morphology of the SAN/LCP blend near the skin region. With the increase of the SAG2 content in the blend, the LCP phase domains become greater in number and are characterized by finer fibrils. Figure 10 shows the effect of GMA content in SAG copolymer on the SAN/LCP blend morphology near the skin region, where the SAG maintains a constant

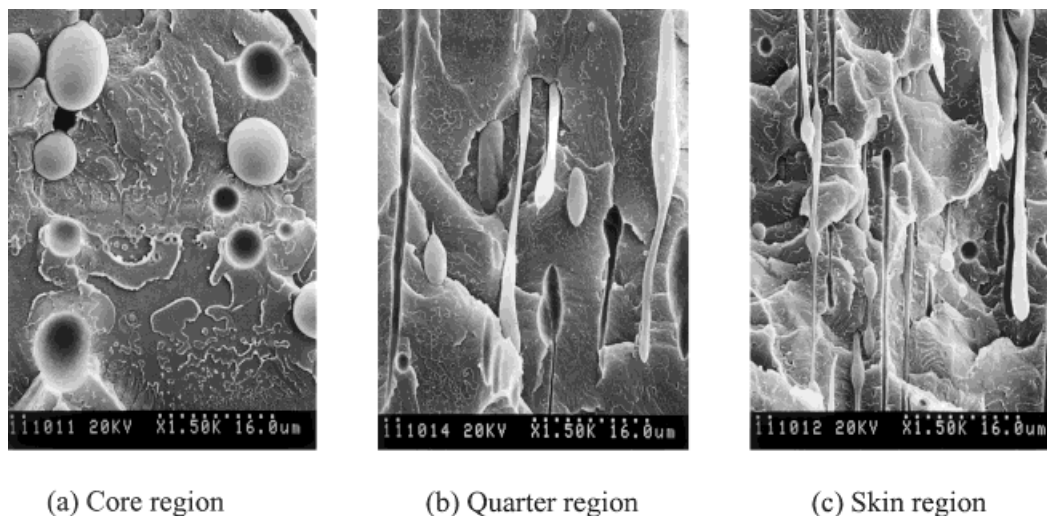


Figure 7 Core-skin SEM micrographs of the cryogenically fractured surfaces of the SAN/LCP (95/5) blends, parallel to the flow direction and at different locations.

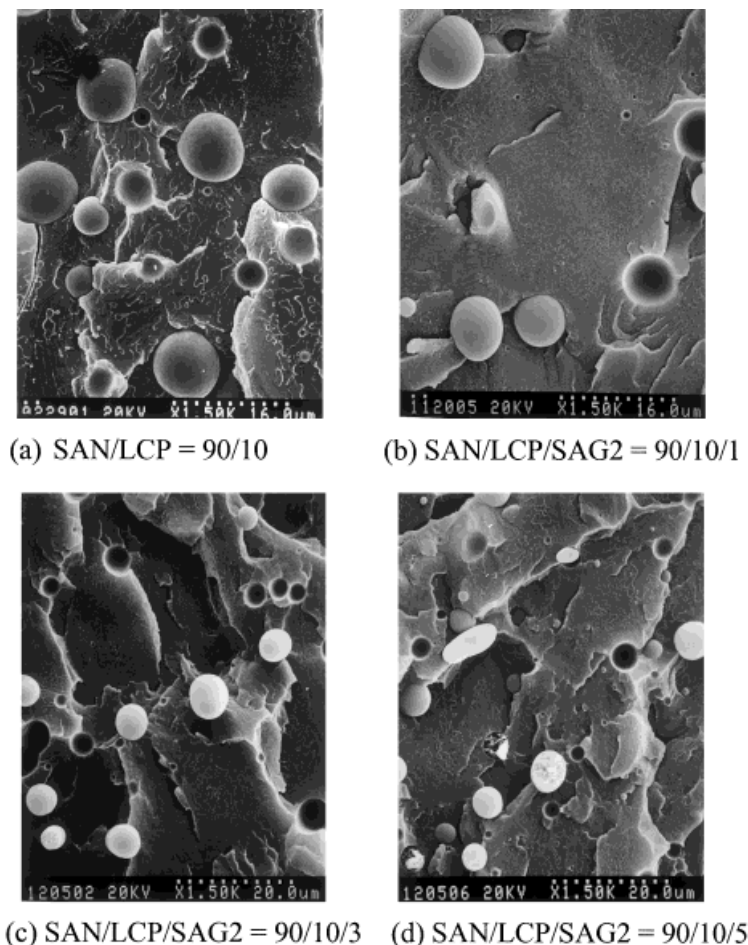


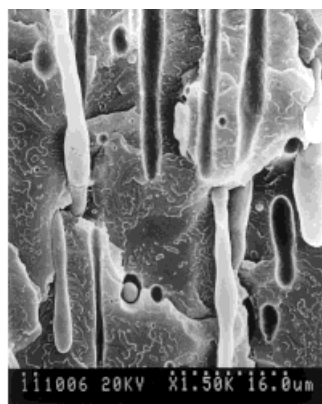
Figure 8 SEM micrographs of the fractured surfaces of the uncompatibilized and compatibilized SAN/LCP (90/10) blends containing varying amounts of SAG2 in the blends, parallel to the flow direction and at the core region.

5 phr in the blend. Comparing Figure 9(d) and Figure 10(a), it is clear that the LCP fibrils show a relatively high aspect ratio for the SAG2 compatibilized blend than that for the SAG5 compatibilizer. Moreover, essentially all the LCP fibrils disappear and small LCP droplets are presented for the SAG8 compatibilized blend [Fig. 10(b)]. Higher GMA content in SAG may produce excessively grafted copolymers, thus decreasing its efficiency as a compatibilizer. Therefore, a minimum LCP content in the blend is necessary to form the LCP fibrils near the skin region. This result is similar to our previously published report on polypropylene (PP)/LCP blends.²⁰

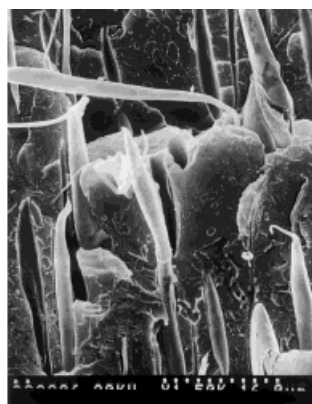
Mechanical Properties

The interfacial properties of blends play an important role in determining the dispersion of the

minor phase and the resultant mechanical performance.^{21–23} The tensile properties and unnotched impact strengths of the SAN/LCP blends for all the compositions in this study are summarized in Table II. For the uncompatibilized SAN/LCP blends, both tensile strength and modulus increase with increasing LCP content. This is the general trend of the mechanical properties for TP/LCP blends when LCP is the minor component in the blend. Figure 11 shows the effect of GMA and SAG content on the impact strength for the SAN/LCP/SAG (90/10/*x*) blends. It is clear that the impact strength of the compatibilized SAN/LCP/SAG2 blends increases consistently with increasing SAG2 content in the blends. As mentioned earlier (Fig. 9), the morphologies of the cryogenically fractured surfaces of the SAN/LCP/SAG2 (90/10/5) blend possess more and finer



(a) SAN/LCP = 90/10



(b) SAN/LCP/SAG2 = 90/10/1



(c) SAN/LCP/SAG2 = 90/10/3

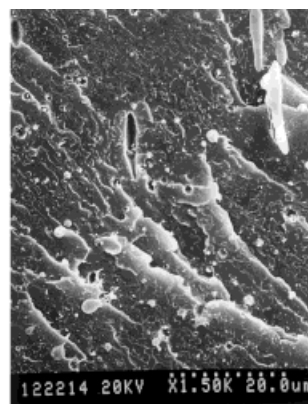


(d) SAN/LCP/SAG2 = 90/10/5

Figure 9 SEM micrographs of the fractured surfaces of the uncompatibilized and compatibilized SAN/LCP (90/10) blends containing varying amounts of SAG2 in the blends, parallel to the flow direction and at the skin region.



(a) SAN/LCP/SAG5 = 90/10/5



(b) SAN/LCP/SAG8 = 90/10/5

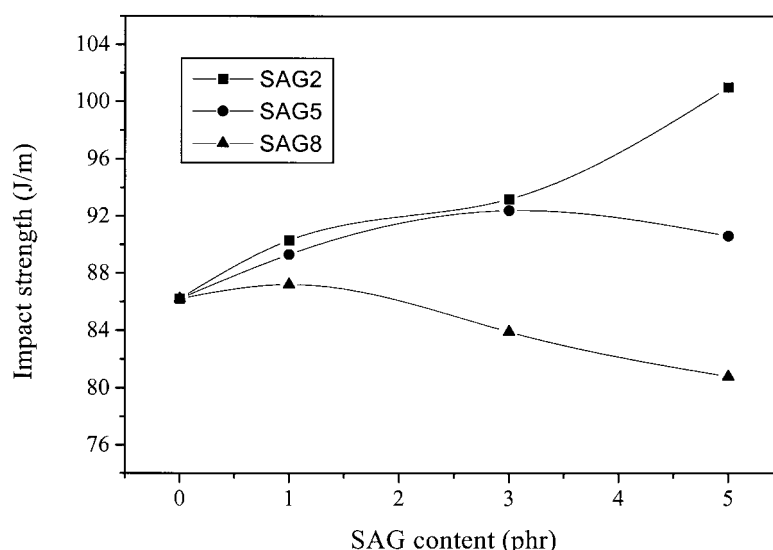
Figure 10 SEM micrographs of the fractured surfaces of the compatibilized (a) SAN/LCP/SAG5 (90/10/5) and (b) SAN/LCP/SAG8 (90/10/5) blends, parallel to the flow direction and at the skin region.

Table II Tensile and Impact Properties of the SAN/LCP Blends

Composition	Tensile Strength (Mpa)	Tensile Modulus (Mpa)	Unnotched Impact Strength (J/m)
SAN/LCP = 100/0	70.7	3400	83.7
SAN/LCP = 95/5	75.9	3680	94.0
SAN/LCP = 90/10	78.2	3810	86.2
SAN/LCP = 80/20	84.6	4260	82.8
SAN/LCP/SAG2 = 90/10/1	84.0	3880	90.6
SAN/LCP/SAG2/Cat = 90/10/1/0.02	90.1	3940	94.3
SAN/LCP/SAG2 = 90/10/3	92.4	3950	93.2
SAN/LCP/SAG2/Cat = 90/10/3/0.02	101.2	3980	97.1
SAN/LCP/SAG2 = 90/10/5	98.4	4080	101.0
SAN/LCP/SAG2/Cat = 90/10/5/0.02	104.5	4100	103.5
SAN/LCP/SAG5 = 90/10/1	83.0	3930	89.3
SAN/LCP/SAG5 = 90/10/3	90.8	3960	92.4
SAN/LCP/SAG5 = 90/10/5	93.2	3940	90.6
SAN/LCP/SAG8 = 90/10/1	84.4	3960	87.2
SAN/LCP/SAG8 = 90/10/3	82.8	3810	83.9
SAN/LCP/SAG8 = 90/10/5	80.2	3620	80.8

fibrils. For the SAN/LCP (90/10) blends with SAG5 compatibilizer, the effect of SAG5 content on the impact strength of the SAN/LCP/SAG5 blends is not very significant. On the contrary, the greater the SAG8 content in the SAN/LCP (90/10) blend, the lower the impact strength. This is because higher GMA content in SAG may produce excessively grafted copolymers, which is considered to be less effective on compatibilization.^{9,12} Figure 12 shows the effect of SAG2 content, with and without catalyst, on the tensile modulus for

the SAN/LCP/SAG2 (90/10/*x*) blends. The compatibilized SAN/LCP/SAG blends, with or without ETPB catalyst, show the same trend, where the tensile modulus increases with increasing SAG2 content in the blend. Both tensile strength and modulus are considered to comprise the material strength, whereas the tensile elongation and impact strength comprise the material toughness. Most of the literature reported that the compatibilized TP/LCP blend results in a decrease in the number of fibrils and tends to convert LCP

**Figure 11** Effect of GMA and SAG content on the impact strength for the SAN/LCP/SAG (90/10/*x*) blends.

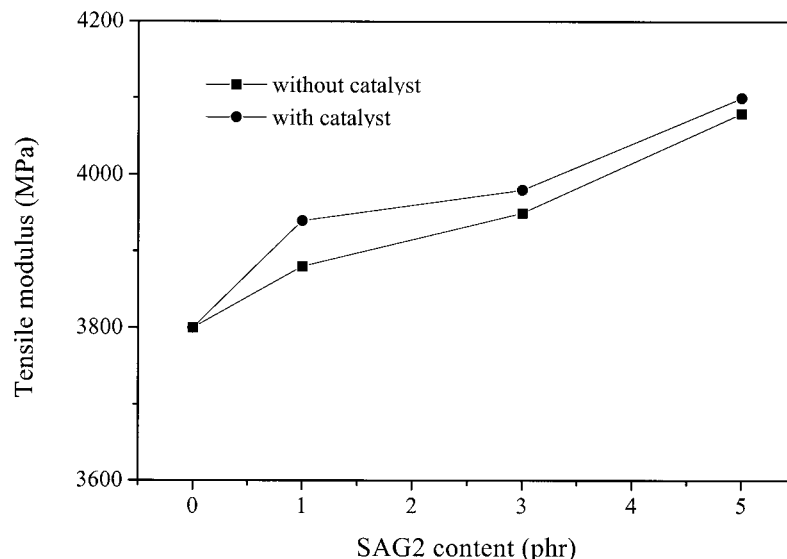


Figure 12 Effect of SAG2 content on the tensile modulus for the SAN/LCP/SAG2 (90/10/*x*) blends.

fibrils to droplet domains. It is unusual for polymeric materials to have both properties, strength and toughness, improved simultaneously through any form of modification. Similar to the results from the Noryl/LCP blends,¹⁴ this study shows both strength and toughness improvements simultaneously after properly controlled compatibilization.

CONCLUSIONS

SAN and LCP comprise an immiscible and incompatible polymer pair in terms of microstructure and mechanical properties. The styrene-acrylonitrile-glycidyl methacrylate (SAG) copolymer was demonstrated to be an effective reactive compatibilizer for the SAN/LCP blend in this study. This SAN-*g*-LCP grafted copolymers tend to anchor along the interface with the ungrafted SAG segments (SAN segments), penetrating into the SAN phase while the branched LCP chains protrude into the LCP phase. For higher GMA content in the SAG (e.g., SAG8), the grafted copolymer is not considered as an effective compatibilizer because the excessively grafted SAN-*g*-LCP copolymer may be drawn into the SAN phase, resulting in fewer LCP fibrils or even forming droplet domains. On the contrary, lower GMA content in the SAG (e.g., SAG2) results in a better compatibilized blend. The reduced interfacial tension makes the LCP phase dis-

perse into fine droplets and then elongates the droplets into fibrils with high aspect ratio during the injection-molding process. The presence of ETPB catalyst promotes the grafting reaction. The variation of the LCP morphology and the increase of the interface adhesion of the compatibilized blends are believed to be responsible for the observed improvements in mechanical properties.

This study was financially supported by the National Science Council, Republic of China.

REFERENCES

1. Baird, D. G.; Wilkes, G. L. *Polym Eng Sci* 1983, 23, 632.
2. Joseph, E. G.; Wilkes, G. L.; Baird, D. G. *Polym Prepr* 1984, 25, 94.
3. da Silva, L.; Bretas, R. E. S. *Polym Eng Sci* 1983, 23, 632.
4. Chin, H. C.; Chang, F. C. *Polymer* 1997, 38, 2947.
5. Li, R.; K. Y.; Tjong, S. C.; Xie, X. L. *J Polym Sci Polym Phys Ed* 2000, 38, 403.
6. Bretas, R. E. S.; Baird, D. G. *Polymer* 1993, 34, 759.
7. Datta, A.; Baird, D. G. *Polymer* 1995, 36, 505.
8. Tjong, S. C.; Li, R. K. Y.; Xie, X. L. *J Appl Polym Sci* 2000, 77, 1964.
9. Maa, C. T.; Chang, F. C. *J Appl Polym Sci* 1993, 49, 913.
10. Chang, D. Y.; Kuo, W. F.; Chang, F. C. *Polym Networks Blends* 1994, 4, 157.

11. Chen, S. H.; Chang, F. C. *J Appl Polym Sci* 1994, 51, 955.
12. Chang, H. H.; Wu, J. S.; Chang, F. C. *J Polym Res* 1994, 1, 235.
13. Lee, P. C.; Kuo, W. F.; Chang, F. C. *Polymer* 1994, 35, 5641.
14. Chang, D. Y.; Chang, F. C. *J Appl Polym Sci* 1995, 56, 1015.
15. Chiou, Y. P.; Chang, D. Y.; Chang, F. C. *Polymer* 1996, 37, 5653.
16. Lu, M.; Keskkula, H.; Paul, D. R. *Polym Eng Sci* 1994, 34, 33.
17. Ju, M. Y.; Chang, F. C. *Polymer* 2000, 41, 1719.
18. Heino, M. T.; Hietaoia, P. T.; Vainio, T. P.; Seppala, J. V. *J Appl Polym Sci* 1994, 51, 259.
19. da Silva, L.; Bretas, R. E. S. *Polym Eng Sci* 2000, 40, 1414.
20. Chiou, Y. P.; Chiou, K. C.; Chang, F. C. *Polymer* 1996, 37, 4099.
21. Sundararaj, U.; Macosko, C. W. *Macromolecules* 1995, 28, 2647.
22. Kim, J. K.; Kim, S.; Park, C. E. *Polymer* 1997, 38, 2155.
23. Zhao, H. Y.; Huang, B. T. *J Polym Sci Polym Phys Ed* 1998, 36, 85.